The structure analysis of the approximant $Ta_{97}Te_{60}$ provides insight into the architecture of quasicrystalline $Ta_{3+2\sqrt{3}}Te_4$ exhibiting twelvefold symmetry

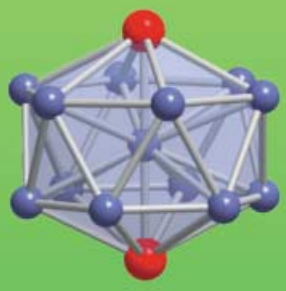

$TaTa_{12}Te_2$ cluster

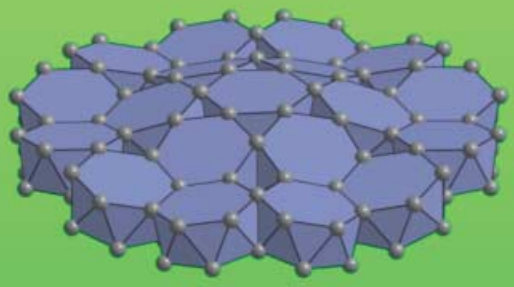

Ta_{151} cluster

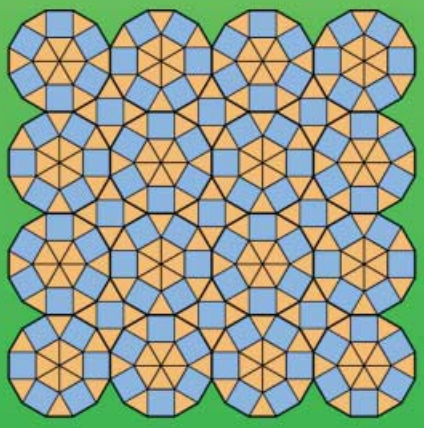

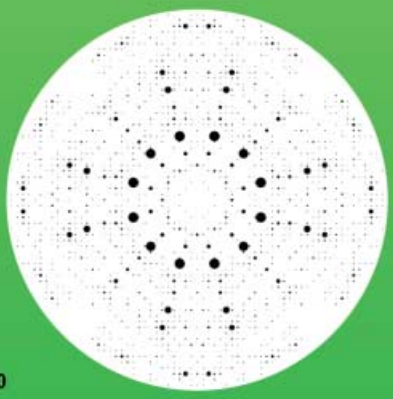

$Ta_{97}Te_{60}$

approximants

quasicrystal

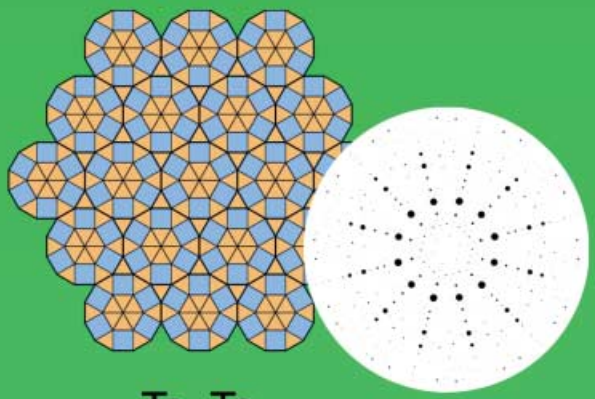

$Ta_{21}Te_{13}$

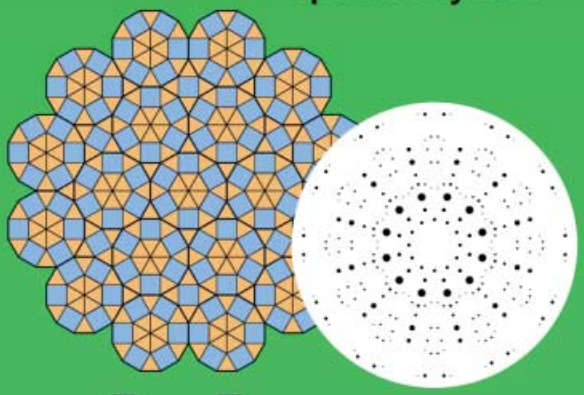

$Ta_{3+2\sqrt{3}}Te_4$

For more information see the following pages.

  0947-6539/02/0814-3093 $ 20.00+.50/0

$Ta_{97}Te_{60}$: A Crystalline Approximant of a Tantalum Telluride Quasicrystal with Twelvefold Rotational Symmetry

Matthias Conrad and Bernd Harbrecht*[a]

Abstract: The crystal structure of a rational approximant of an unprecedented dodecagonal quasicrystal is reported. The atomic arrangement of the tantalum-rich telluride $Ta_{97}Te_{60}$ has been determined from 30458 symmetrically independent X-ray intensities of a crystal twinned by metric merohedry: $a = 2767.2(2)$, $b = 2767.2(2)$, $c = 2061.3(2)$ pm, space group $P2_12_12_1$, Pearson symbol $oP628$, 1415 variables, $R(F) = 0.059$. A dodecagonal-shaped, vaulted $Ta_{151}Te_{74}$ cluster with maximum symmetry $6mm$ can be seen as a characteristic motif of the structure. Each cluster measures about 2.5 nm across and consists of nineteen concentrically condensed hexagonal antiprismatic Ta_{13} clusters which are capped with Te atoms. The $Ta_{151}Te_{74}$ clusters can cover the plane distinctly in different ways, thereby forming a series of phases which are closely related both structurally and compositionally. In $Ta_{97}Te_{60}$ the buckled clusters decorate the vertices of a square tiling at a 2 nm length scale to result in corrugated lamellae $^2_\infty[Te_{30}Ta_{41}Ta_{15}Ta_{41}Te_{30}]$ each about 1 nm thick. The lamellae are stacked along the c axis, corresponding to the direction of the pseudo-twelvefold axis of symmetry. Symmetry arguments are proposed that the twinning of the structure may be associated with a fine-tuning of weak interlayer Te – Te interactions which are reflected in a minimization of the deviation from the mean distance $\langle d_{Te-Te} \rangle$ and a doubling of the stacking vector $\boldsymbol{c}$.

Keywords: crystalline approximant · high-temperature synthesis · quasicrystal · tantalum · tellurium

Introduction

Quasicrystals represent a particular state of condensed matter that differs from known standards in terms of order and symmetry. The signature of quasicrystals is a diffraction image with discrete intensity maxima and a rotational symmetry that is incompatible with basic laws of classical crystallography.[1] Quasicrystals may give rise to diffraction images with five-, eight-, ten- or twelvefold rotational symmetry. They are classified according to their symmetry.[2] The sharp diffraction spots irrefutably prove that the atoms are highly ordered on a length scale that is much larger than the interatomic distances. On the other hand, the crystallographic forbidden rotational symmetry of the Fourier spectrum expresses a unique mode of long-range order in the quasicrystalline state that cannot result from a repetition of atoms at given distances in distinct directions of physical space as is typical of ordinary crystals. Quasicrystals do not possess this kind of plain translational symmetry.

Structure determination techniques for solids usually rely on the translational periodicity of crystals. Hence, these methods fail for quasicrystals. Therefore, the precise structure analysis and description of a quasicrystal structure is a not a trivial task. Various methods have been proposed to overcome the problems associated with the lack of translation invariance.[3] For example, the embedding method is based on the assumption that the atoms in quasicrystals are periodically arranged as in ordinary crystals, albeit in a space with more than three dimensions.[3f,g] This premise has the advantage that the concepts and tools of higher-dimensional crystallography can be applied to solve and describe the structures of quasicrystals.[2] Other methods providing essential information about the quasicrystalline state are electron diffraction and high-resolution transmission electron microscopy. Structures are modeled by decorating quasiperiodic tilings and coverings with atoms.[4] A more conventional approach makes use of the fact that quasicrystals usually form in close proximity to phases with related periodic structures, so-called rational or crystalline approximants. The intimate structural relationship between a quasicrystal and its approximants is concluded from a strong resemblance in the intensity distribution of the diffraction images. Apparently, the noncrystallographic rotational symmetry of the quasicrystal is relinquished in the crystalline approximants in favor of the restoration of ordinary translational periodicity. Therefore, the study of approximant structures can meaningfully contribute to the understanding of the nature of the quasicrystalline state, in particular as long as the determination of the structure of the respective quasicrystal has not yet been accomplished.

In the following, we report on the structure of the tantalum-rich telluride $Ta_{97}Te_{60}$, one of the approximants of an

[a] Prof. Dr. B. Harbrecht, Dr. M. Conrad
Department of Chemistry and Materials Science Center
Philipps University, 35032 Marburg (Germany)
Fax: (+49) 6421-2828917
E-mail: harbrecht@chemie.uni-marburg.de

  0947-6539/02/0814-3094 $ 20.00+.50/0

unprecedented quasicrystalline chalcogenide that we discovered recently.[5] The Fourier spectrum of $Ta_{1.6}Te$ exhibits twelvefold rotational symmetry. This telluride belongs to the class of so-called dodecagonal quasicrystals. Dodecagonal phases were identified in the Cr–Ni,[6] Ni–V(–Si),[7] Bi–Mn,[8] Mn–Si[9] and Ta–Te[5] systems. The tantalum telluride is the thermally most robust among these dodecagonal phases. Quite untypical for all other known quasicrystals, the dodecagonal telluride has lubricant-like properties. The crystal structure of the approximant $Ta_{97}Te_{60}$ provides strong evidence that the particular mechanical properties of the quasicrystalline telluride are intimately associated with a lamellar structure that exhibits strong interatomic interactions in only two dimensions. As schematically shown in Figure 1, the similar intensity distributions of the zero-order precession photographs of the quasicrystalline and the approximant phase corroborate the assumption of a strong resemblance of both structures.

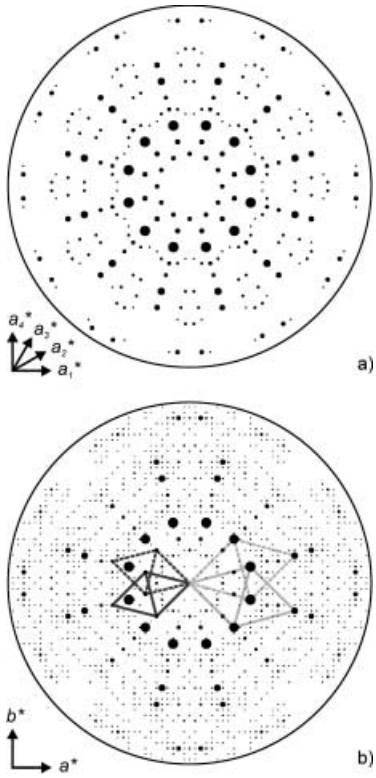

Figure 1. X-ray intensity distribution in the zeroth layers perpendicular to the (pseudo-) twelvefold symmetry axes for a) dd-$Ta_{1.6}Te$ (estimated intensities from Buerger precession photographs) and b) its approximant $Ta_{97}Te_{60}$ (IPDS data). The observed intensity is proportional to the area of the circles. Note that the diffraction image of the approximant shows additional weak reflections which are arranged on a reciprocal square lattice thereby breaking the twelvefold symmetry. For details, see section on "structural properties".

Results and Discussion

Heavily corrugated lamellae, each about one nanometer across, comprise the distinctive layer-type structure of $Ta_{97}Te_{60}$. Each lamella consists of five atom layers, the outer two of which are composed of Te atoms. Strong Ta–Te (mean value $\langle d \rangle = 305$ pm) and homonuclear Ta–Ta bonding interactions ($\langle d \rangle = 295$ pm) are confined to such quasi-two-dimensional structural units. In accordance with the lubricant-like mechanical properties of this metal-rich telluride, the cohesion of the lamellae seems to be mainly the result of weak Te–Te interactions ($d_{Te-Te} \geq 334$ pm). There are two lamellae per unit cell symmetrically coupled by a 2_1 screw rotation. They are stacked along *c*. A projection of a suitable part of two lamellae cut out along [110] is shown in Figure 2a)

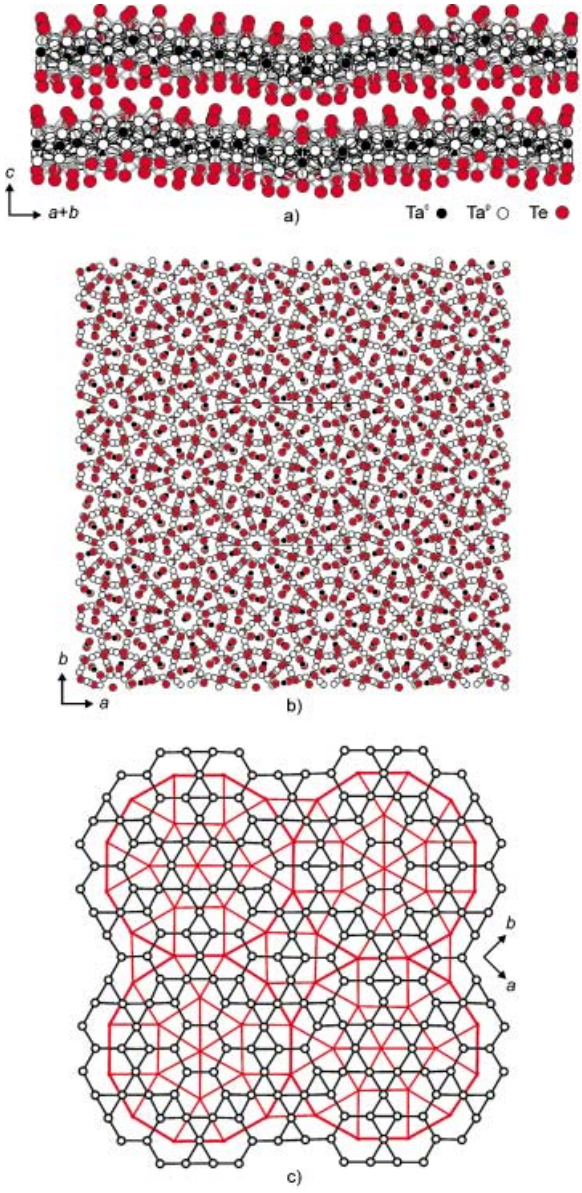

Figure 2. a) Projection of a suitable section of the crystal structure of $Ta_{97}Te_{60}$ onto $(1\bar{1}0)$ with emphasis on the corrugation of the lamellae and the contacts between weakly bonded Te atoms of adjacent layers. Filled black circles: Ta^c atoms in the interior secondary net; open circles: Ta^p atoms in the primary nets; red circles: Te atoms in the two outermost layers of a lamella. b) Projection of a lamella onto (001). It is composed of one Ta^c (black filled circles), two Ta^p (black open circles), and two Te (red circles) layers. c) Net representation of the Ta partial structure of $Ta_{97}Te_{60}$. The Ta^p atoms are arranged in layers corresponding to an irregular hexagon/triangle net (black). The Ta^c net below the hexagons of the Ta^p net forms an irregular square/triangle net (red). For the sake of clarity, the second primary net, which is rotated by 90° relative to the first one, is left out.

In the following, we show that the pseudododecagonal symmetry of the structure essentially results from the arrangement of atoms within the atomic layers and the specific orientation of these layers within a lamella. Accordingly, the pseudo-twelvefold rotational symmetry underlying the approximant structures is reflected in global rather than in local structural features. To emphasize this aspect, we have split the structure into nets by using and extending a concept that has been successfully applied by Frank and Kasper for a thorough analysis of a series of complex intermetallic structures.[10a,b, 11] Moreover, we have elucidated existing structural relations between the various approximants. For this purpose we employed the concept of condensed clusters[12] in an extended version.

The lamellae of the structure of $Ta_{97}Te_{60}$ consist of five atom layers with distinct compositions and orientations, namely $\Delta Te_{30} - \nabla Ta^{p}_{41} - Ta^{c}_{15} - \Delta Ta^{p}_{41} - \nabla Te_{30}$. A loosely packed central net of Ta^{c} atoms is surrounded by two peripheral layers of Ta^{p} atoms. The nets of Ta atoms are covered on both sides by densely packed layers of Te atoms of hexagonal topology 3^6. The Schläfli symbols, for example 3^6 or $3^2.4.3.4$, indicate the vertex configurations of the respective net; the bases signify the type of polygons about a vertex of the net and the exponents express the number of the respective polygons surrounding a given vertex of the net. Accordingly, 3^6 indicates the Te atoms being arranged to triangles of which six are grouped around each vertex. The mean distance between a Te atom and its six nearest neighbors within a layer is 397 pm.

The peripheral Ta atoms are also situated at the vertices of distorted hexagonal nets. In this case, however, 30 out of the 112 vertices per unit cell are unoccupied. Thus, the Ta^{p} atoms form irregular nets of triangles and hexagons. The polygons are locally arranged in three distinct ways: the three vertex configurations 6^3, 6.3.6.3, and $6^2.3^2$ occur in the ratio 8:14:19. The Ta atoms of these primary nets are strongly bonded to each other. Each atom has three or four bonding contacts at a mean distance $\langle d \rangle = 287$ pm. The layers of Te and of Ta^{p} atoms are symmetrically related pairwise by 2_1 screw rotations. The corresponding symmetry axes run parallel to b within a lamella. Since the edges of the nets are rotated by $\approx 15^\circ$ relative to b, the respective pairs of layers are in antiparallel orientation as indicated by the symbols ∇ and Δ in the above scheme. The Ta^{p} atoms of adjacent layers are also in close contact ($\langle d \rangle = 291$ pm). The topology of the layers and their relative orientation to each other is quite distinctive: all hexagons are antiprismatically stacked on top of each other. Pairs of superimposed hexagons offer space for Ta^{c} atoms in between the Ta^{p} layers. The Ta^{c} atoms are arranged to a less-densely packed layer, a so-called secondary layer. These atoms are not in close contact with each other and the mean distance between central Ta atoms within a net is 528 pm. The Ta^{c} atoms occupy the vertices of an irregular square/triangle tiling with two distinct vertex configurations 3^6 and $3^2.4.3.4$ occurring in the ratio 1:14. Figure 2b shows the projection of a lamella and Figure 2c one secondary and one primary net of Ta atoms onto [001].

The nets of hexagonal topology that compose the structure of $Ta_{97}Te_{60}$ are reflected in the Fourier spectrum. Figure 1b shows that the strong reflections of the ($hk0$) section of the reciprocal lattice—that is, the Fourier transform of the structure projected onto the plane perpendicular to the pseudo-twelvefold symmetry axis—define the nodes of two pairs of nets of approximately hexagonal shape. In principle, the two nets of each pair can be transformed into each other by a rotation of $\approx 30^\circ$. The edge lengths in real space amount to 383 and 281 pm. The strongest reflections accumulate at the nodes of the bigger hexagonal nets. In real space the distance in the net corresponds to the projection of the heavily scattering Ta atoms located in a secondary and one of the two primary nets onto the a/b plane.

This description of the $Ta_{97}Te_{60}$ structure sheds light on the origin of its pseudododecagonal character. Accordingly, the dodecagonal signature of the long-range order in $Ta_{97}Te_{60}$ results from the arrangement of the Te and Ta^{p} atoms in layers of approximately hexagonal rotational symmetry in combination with a pairwise coupling of the layers by a pseudo-fourfold rotoinversion. The dodecagonal characteristic is transcribed into the secondary tiling defined by the Ta^{c} atoms. They mark exactly those positions in the projection onto the a/b plane for which the two antiparallel primary hexagonal nets underlying the Ta^{p} atom layers superimpose almost perfectly.

The orientation of the edges of the secondary tiling provides a suitable measure to quantify the deviation from a perfect twelvefold long-range orientation order. In a truly dodecagonal structure, the six distinct directions of the edges of a regular dodecagon occur with the same frequency. In the secondary tiling of $Ta_{97}Te_{60}$ they are found in the ratio 7:6:6:7:6:6. The preferred orientation corresponds to [110] and symmetry-related directions.

From a local point of view, the approximation of dodecagonal long-range order in $Ta_{97}Te_{60}$ becomes manifest in slightly distorted dodecagons that almost completely pave the area of the secondary tiling (Figure 2c). Each dodecagon consists of twelve triangles and six squares and is linked to four others by edge-to-edge connections. The centers of the dodecagons coincide with the subset of the 3^6 vertices of the secondary tiling. This particular subset defines a regular 4^4 tiling, which—in extension of the concept of Frank and Kasper[10a,b]—we call a tertiary tiling. The edge length of the tiling is given by the distance of two opposite edges of a dodecagon, namely $a/\sqrt{2} = 1952$ pm. This spacing equals the sum of two times the sum of the edge length of a square plus the height of a regular triangle of the secondary tiling, as can be seen from the red net depicted in Figure 2c. Thus, the ratio of the mean edge lengths of the secondary and tertiary tiling underlying the structure of this dodecagonal approximant matches the value $2 + \sqrt{3}$, which is equal to the irrational scale factor of quasiperiodic dodecagonal tilings.[13]

At a first glance, the structure seems to be rather complex. There are 157 crystallographic distinct atoms, see Table 1. The analysis of the local coordination configurations, however, reveals that topological criteria allow the reduction of the number of topologically nonequivalent atoms down to six. The various coordination polyhedra about the three distinct types of Ta atoms are shown in Figure 3a. The Ta^{c} atoms (Ta1 – Ta15) of the interior layer have a coordination number of fourteen. Twelve Ta^{p} atoms form a hexagonal antiprism

  0947-6539/02/0814-3096 $ 20.00+.50/0 *Chem. Eur. J.* **2002**, *8*, No. 14

Table 1. Crystallographic data and structure determination.

formula	$Ta_{97}Te_{60}$
space group	$P2_12_12_1$
pearson symbol,	*oP*628
Z	4
a [pm]	2762.7(2)
b [pm]	2762.7(2)
c [pm]	2061.3(2)
$V \times 10^6$ [pm^3],	15734(2)
μ [mm^{-1}]	78.00
formula weight [g mol^{-1}]	25208.15
ρ_{calcd} [g cm^{-3}]	10.642
data collection	
crystal size [μm]	$220 \times 180 \times 20$
radiation, monochromator	$Mo_{K\alpha}$, graphite
ϕ range [°]/ϕ increment [°]	161/0.7
θ (min/max) [°]	1.7/26.1
reflections	101018
data reduction	
programs	IPDS,[24] SHELX 93[25]
absorption correction	numerical
transmission range	0.002–0.246
unique reflections	30895
$R_{int}(F^2)$, completeness of data set	0.099, 0.988
refinement	
program	SHELX 93[25]
reflections observed	30458
variables	1415
$R_w(F^2)/R(F)$ for 25451 reflections $[F^2 > 2\sigma(F^2)]$	0.129/0.059
GOF	1.12
residual electron density (min/max) [10^{-6} e pm^{-3}]	−5.0/5.7
twin operation/fraction	$(-y, x, -z)$/0.531(1)

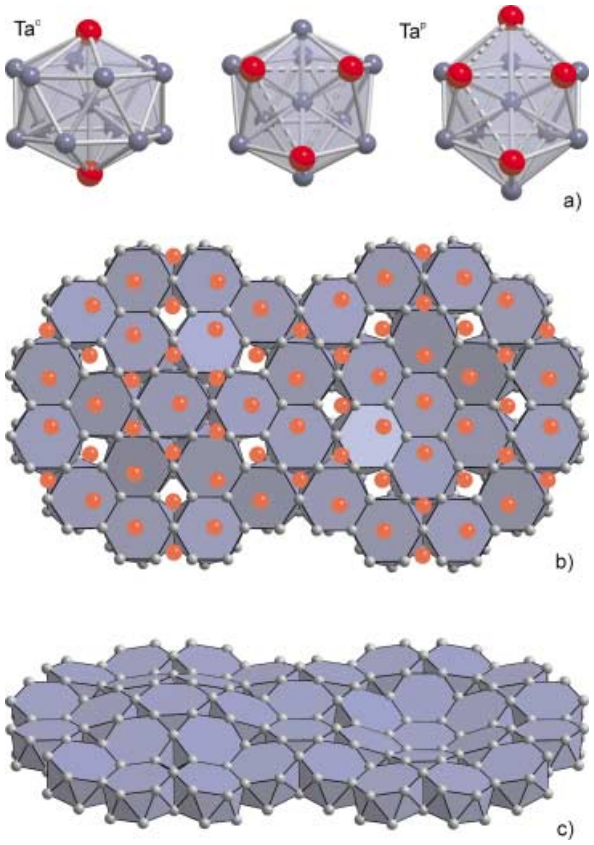

Figure 3. a) The three chemically distinct coordination types for Ta in $Ta_{97}Te_{60}$. b) Projection onto (001) and c) side view of two partly overlapping vaulted Ta_{151} units composed of 19 concentrically fused hexagonal antiprismatic $TaTa_{12}$ clusters covered by Te atoms (red circles) in b).

($\langle d_{Ta-12Ta}\rangle = 312$ pm) around Ta^c with two additional Te atoms capping the hexagonal faces, $\langle d_{Ta-2Te}\rangle = 277$ pm. Though all Ta^p atoms have a distorted icosahedral coordination, two forms can be distinguished. Ta16–Ta59 are surrounded by nine Ta ($\langle d_{Ta-9Ta}\rangle = 294$ pm) and three Te atoms ($\langle d_{Ta-3Te}\rangle = 300$ pm). The atoms Ta60–Ta97, which are located above the edges of the secondary tiling, have eight Ta ($\langle d_{Ta-8Ta}\rangle = 295$ pm) and four Te atoms ($\langle d_{Ta-4Te}\rangle = 316$ pm) as next neighbors. Owing to the layer-type character of the structure of $Ta_{97}Te_{60}$, all Te atoms covering the surfaces of the lamellae coordinate Ta atoms only from one side. The atoms Te1–Te30 are situated above the vertices of the secondary tiling and are close to seven Ta atoms ($\langle d_{Te-7Ta}\rangle = 316$ pm). The atoms Te31–Te47 cap the triangles of the secondary tiling, $\langle d_{Te-3Ta}\rangle = 283$ pm. The third type of Te atoms, Te47–Te60, are located above the squares of the secondary tiling, $\langle d_{Te-4Ta}\rangle = 289$ pm.

Starting from the coordination of the atoms, the architecture of the metal partial structure of $Ta_{97}Te_{60}$ and related tellurides can be described elegantly and consistently by means of a modular cluster concept. As can be seen from Figure 2c, the tantalum core of the extended lamellar structural unit $^2_\infty[Te_{30}Ta^p_{41}Ta^c_{15}Ta^p_{41}Te_{30}]$ corresponds to a condensate of a single cluster type, namely the above-mentioned hexagonal antiprismatic $Ta^cTa^p_{12}$ unit. Clusters of this type share triangular faces with adjacent Ta_{13} units. Consequently, the Ta_{13} clusters situated at the 3^6 vertices are connected to six clusters, whereas the outer six share faces with five clusters. The result is a dodecagonal Ta_{151} cluster representing an agglomeration of 19 concentrically arranged Ta_{13} clusters. Its size determines the edge length of the tertiary tiling and the central atoms of the dodecagonal-shaped clusters fix the tertiary tiling.

These large clusters may be arranged exclusively into squares, as found for $Ta_{97}Te_{60}$, or into triangles, as derived for $Ta_{21}Te_{13}$.[14e] For $Ta_{181}Te_{112}$, the Ta atoms at the centers of the Ta_{151} clusters define a semiregular tertiary square/triangle tiling of configuration $3^2.4.3.4$.[14a] The tiling underlying a truly dodecagonal phase is irregular and aperiodic. In this particular case, the ratio of triangles and squares is $4/\sqrt{3}$, each type of tile covers half of the area.

Two further aspects should be emphasized: 1) the highest possible symmetry of the Ta_{151} cluster constituting the structures of the dodecagonal approximants is 6*mm*. In all known approximant structures of dd-$Ta_{1.6}Te$ (dd = dodecagonal) the symmetry group of the cluster is a subgroup of 6*mm*. Note that 82 out of 97 Ta atoms of the pseudododecagonal structure of $Ta_{97}Te_{60}$ have a distorted icosahedral coordination. Thus, the symmetry of a quasicrystal does not necessarily result from a constituting structural unit with the appropriate noncrystallographic symmetry. In the case of dd-$Ta_{1.6}Te$, the dodecagonal symmetry reflects a particular global rather than a local structural feature. 2) The metal substructure of a lamella of $Ta_{97}Te_{60}$ can be considered as a suitable section of a hypothetical tetrahedral close-packed intermetallic phase, that is, a structure in which all metal atoms are arranged into tetrahedra. A structure of this type would be assigned to a particular family of Frank–Kasper phases. For example, the σ[11], H,[15] and F phases,[16] belong to this family. Our hypothetical structure could be seen as a chemical inter-

growth of motifs present in the structures of Cr_3Si[17] and Zr_4Al_3,[18] two other representatives of this family. The common feature of all these phases is a secondary square and/or triangle tiling whose vertices coincide with the centers of hexagonal antiprismatic metal clusters. For intermetallic phases of this family, the clusters are not only condensed into layers, as for the telluride, but also arranged to columns by sharing hexagonal faces. The dodecagonal quasicrystalline phases uncovered in the Cr–Ni[6] and Ni–V(-Si)[7] systems probably share this structural feature.

A striking feature of the structure of $Ta_{97}Te_{60}$ is the heavy corrugation of the lamellae. The buckling is best seen in Figure 2a, in which two ribbons have been cut out from adjacent lamellae. Within the primary Ta^p layer, the amplitude of the wave is $\approx$170 pm. In the outer Te layers, the corrugation is slightly enhanced. Hence, the Te atoms fluctuate in height by nearly 400 pm. The extremities of the buckled layer spread around the 3^6 vertices of the secondary tiling coinciding with the centers of the bell-shaped Ta_{151} clusters (Figure 3c). The curvature inverts between adjacent clusters which are symmetrically coupled by 2_1 screw rotation with the corresponding symmetry axes running parallel to *b*. The corrugation itself originates from the specific way in which the Ta_{13} clusters sharing triangular faces are fused together. It is an inherent feature of a hexagonal antiprism that the triangular faces are not perpendicularly arranged relative to the hexagons. Thus, at low degrees of distortions of the antiprismatic Ta_{13} clusters, the Ta framework cannot be flat. The specific topology of its corrugation with extremities at the centers of the Ta_{151} cluster is intrinsically connected with the concentric condensation of the hexagonal antiprismatic Ta_{13} clusters.

All structural features elucidated so far are in accordance with a tetragonal space group symmetry. The arrangement with the highest possible symmetry compatible with the topology of the structure of $Ta_{97}Te_{60}$ could be described in space group $P\bar{4}2_1m$. As a consequence, the lamellae would be equivalent by translation. According to the group–subgroup relationship of the sequence given in Scheme 1, $P\bar{4}2_1m$ is a supergroup of the orthorhombic space group symmetry of the relaxed $Ta_{97}Te_{60}$ structure. The crystal chemical implications of the symmetry reduction on the structure of $Ta_{97}Te_{60}$ are of interest, since subtle symmetry changes may offer a clue to an improved understanding of chemical bonding in the respective solid.

$P\bar{4}2_1m$
↓ t(2)
$P2_122_1$ ($P2_12_12$)
↓ k(2) $\underline{c}' = 2\underline{c}$
$P2_12_12_1$ ($P2_12_12_1$)

Scheme 1.

The reduction of symmetry has a discernible impact on the approximant structure, both with respect to the corrugated lamella $^2_\infty[Te_{30}Ta_{97}Te_{30}]$ and to the stacking of these units. Lowering the symmetry activates some degrees of freedom within the lamellar unit to provide space for an additional differentiation of covalent bonding interactions. For the purpose of a rigorous symmetry analysis of these changes concerning exclusively the lamellar unit, we assume the series of layer groups[19, 20] to be in the group–subgroup relationship given in Scheme 1. From the sequence given in Scheme 2, it becomes evident that both transitions, translationengleich and klassengleich, each contribute to the lowering of the eigen symmetry of the lamellar unit. Indeed, the atomic coordinates within such a unit are shifted on an average by approximately 14 pm relative to the ideal positions of an atomic arrangement with tetragonal symmetry.

$P(\bar{4})2_1m$
↓ t(2)
$P2_122_1(2)$
↓ t(2)
$P12_1(1)$

Scheme 2.

The second transition (klassengleich) in Scheme 1 affords a further degree of freedom that permits a shift of adjacent lamellar units. Indeed, taking the highest Patterson peak in the section $uv\frac{1}{2}$ as a measure, the two next lamellae are shifted relative to each other by $\approx$70 pm. This distortion mainly affects the weak Te–Te interactions between the lamellae. A detailed analysis of these contacts depending upon the relative position of two consecutive lamellae turns out to be complex. One cause is the misfit between adjacent Te layers. The misfit itself is traced back to the antiparallel orientation of the two Te nets of hexagonal topology. The heavy corrugation of the surface of the $[Te_{30}Ta_{97}Te_{30}]$ lamellae is another reason. It follows directly from the geometry of the corrugation that the highest possible filling of space is reached when the stacking of the lamellae is close to primitive. A primitive stacking affords a good match of convex and concave vaulted clusters in consecutive lamellae.

In order to critically examine the factors distinguishing the particular position relation of adjacent lamellae in the structure of $Ta_{97}Te_{60}$, we performed a numerical analysis of the interlayer Te–Te contacts for small displacements of the Te layers from their energetically most favorable positions. Figure 4 shows a contour map of the mean deviation Δd of the

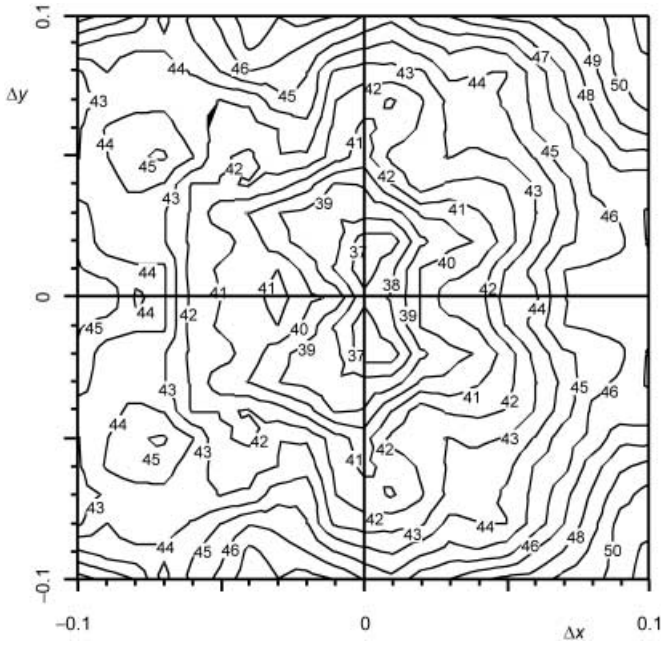

Figure 4. Contour map showing the deviation Δd of the interlayer Te–Te mean distances as a function of the displacement $\Delta r = \Delta \cdot a + \Delta y \cdot b$ of two adjacent lamellae from their position in the distorted structure. Values of Δd are given in pm. Note that Δd is minimal for the relaxed structure, namely, $\Delta r = 0$.

0947-6539/02/0814-3098 $ 20.00+.50/0 *Chem. Eur. J.* **2002**, *8*, No. 14

Te–Te distances from its mean value as a function of the displacement vector $\Delta x \cdot a + \Delta y \cdot b$. Distances up to 500 pm are taken into account. The analysis reveals that the position relation of adjacent Te layers in the orthorhombic distorted structure of $Ta_{97}Te_{60}$ is quite specific: the situation in the relaxed structure is marked by a particularly narrow distribution of the Te–Te distances, namely, Δd is minimal as it may be expected for optimized, nondirectional, attractive Te–Te interactions.

The concluding comment concerns the twinning of the structure. The observation that the twin domains are about of the same size points to the possibility that the twinning is associated with a phase transformation that occurs when the crystal cools down to ambient temperature. Two other findings provide support for this hypothesis: 1) The metric of the twinned orthorhombic crystal satisfies the restrictions of the tetragonal crystal family within the experimental resolution. 2) The structures of the twin domains were found to be related by a rotation inversion. This is exactly the symmetry operation that has to be added as a generator to those of the symmetry group $P2_12_12_1$ of the relaxed structure in order to get to $P\bar{4}2_1m$, the space group of the aristo-type structure. The last two statements are compatible with the assumption that $P\bar{4}2_1m$ is the symmetry group of $Ta_{97}Te_{60}$ at high temperature. The existence of a high-temperature modification, however, has yet to be proven.

Conclusion

The reduction of $TaTe_2$ in the presence of excess tantalum at about 1900 K leads to $Ta_{97}Te_{60}$, a crystalline approximant of a unique dodecagonal quasicrystalline telluride, which forms readily at lower temperatures under otherwise similar conditions.

A comprehensive analysis of the crystal structure of $Ta_{97}Te_{60}$ by its decomposition into distinct sets of atom layers affords insight into the structural principles underlying the architecture of the phase. Most of the atoms are located at the vertices of corrugated triangular nets that are oriented pairwise in an antiparallel fashion giving rise to a pseudododecagonal character of the structure. The coordination about a subset of Ta atoms defining a less densely packed layer at a second level of structural hierarchy can be used to build the structure following a modular cluster concept. A 2.5 nm-wide dodecagonal-shaped, vaulted $Ta_{151}Te_{74}$ cluster was identified as a characteristic motif of the structure. The centers of these clusters define a net at a third level of hierarchy at which the differentiation between the various structures of this unique class of compounds becomes evident.

The intimate knowledge of the approximant structure of an unprecedented dodecagonal quasicrystal provides relevant structural information about other possible approximant structures as well as that of the quasicrystal itself. This knowledge is an indispensable prerequisite for a fundamental understanding of the interrelations between structure and composition for the phases of this unique class of compounds.

Experimental Section

Preparation and characterization: The binary Ta–Te system accommodates a dodecagonal quasicrystalline phase among a series of compositionally and structurally closely related crystalline approximants.[5b, 14] Three of these phases were identified as $Ta_{21}Te_{13}$,[14e] $Ta_{181}Te_{112}$, and $Ta_{97}Te_{60}$.[5b, 14a,b] $Ta_{97}Te_{60}$ is the approximant richest in tantalum. It marks the boundary to the Te-saturated bcc solid solution $Ta_{1-x}Te_x$. It readily forms as the final product of the stepwise reduction of $TaTe_2$ by the metal in sealed tantalum ampoules at temperatures above 1870 K. Lower reaction temperatures and otherwise similar reaction conditions yield dd-$Ta_{1.6}Te$. $Ta_{97}Te_{60}$ was produced from a proper, prereacted, compressed mixture of the elements (Ta powder: Aldrich 99.9%, H. C. Starck, Te pieces: Fluka 99.999%), (silica tube, 1100 K, 1 h) in a sealed tantalum crucible (Plansee) at 1870 K within 12 h. Crystals of improved quality were obtained with otherwise equivalent reaction conditions by adding traces of iodine to the pellet. The plate-shaped crystals exhibit a metallic luster. The crystals split easily parallel to their large faces, that is, perpendicular to *c*. By considering the intensities calculated from the structural parameters, 66 reflections of a Guinier pattern (FR552, Enraf-Nonius, Delft, NL; $Cu_{K\alpha 1}$; *d* values >158 pm) of microcrystalline $Ta_{97}Te_{60}$ were consistently indexed. A tetragonal lattice was assumed, since no splitting of the reflections as a result of orthorhombic translational symmetry was observable. Least-square refinement led to $a = 2758.3(3)$ and $c = 2059.6(3)$ pm. EDX analyses were performed in a transmission electron microscope (CM30ST, Philips, 300 kV) equipped with a Tracor Voyager System. Ta_2Te_3[26] was used as a standard. Averaging of 35 analyses resulted in a molar fraction $x_{Ta} = 0.629(3)$. No further elemental component besides Ta and Te was detected within the accuracy of the method.

Structure analysis: Several crystals were sealed in glass capillaries and examined with a Buerger precession camera. A crystal of dimensions $0.2 \times 0.1 \times 0.02$ mm was chosen for data collection with an imaging plate diffraction system (IPDS, Stoe). Details concerning the data collection are summarized in Table 1. Both photographic and diffractometer data were consistent with a primitive tetragonal space group of Laue class 4/*mmm*. The extinctions in the zones $h00{:}h \neq 2n$, $0k0{:}k \neq 2n$, $00l{:}l \neq 2n$ pointed to the space group $P4_22_12$. All attempts to derive a chemically reasonable structure model by means of direct methods (SHELXS[21], multan[22]) failed. Further useful pieces of information were gained from a systematic inspection of the intensity distribution within the reciprocal layers (*hk*0) and the Patterson sections (*uv*0) of $Ta_{97}Te_{60}$ and $Ta_{181}Te_{112}$, another unsolved approximant structure at this stage. The intensity distribution suggested a principal relationship between the structures of the pseudo-dodecagonal tantalum tellurides and those of a class of Frank–Kasper phases[10] that are intermediate between the Cr_3Si type[17] and the Al_4Zr_3 type[18] structures as, for instance, the structure of the σ phase.[11] The results of high-resolution transmission electron microscopy (HRTEM) studies of both approximants corroborated the assumed structural resemblance. Hereafter, we were able to derive a realistic model for the tantalum partial structure of $Ta_{97}Te_{60}$. A detailed description of the procedure is given elsewhere.[5b]

The space group with maximum symmetry matching the model structure was $P\bar{4}2_1m$, $c' = c/2$. This symmetry, however, did not seem to be compatible with the experimental findings. Discrepancies were attributed to possible twinning and could be resolved by applying an appropriate symmetry reduction taking group–subgroup relations into account. The Patterson section (*uv*½) clearly revealed features indicative for twinning. As shown in Figure 5, the section can be seen as a superposition of four copies of the (*uv*0) section which are specifically shifted to each other. This particular feature led to the conclusion that, according to the symmetry reduction explicitly given in a former paragraph, the proper symmetry of $Ta_{97}Te_{60}$ is to be orthorhombic, $P2_12_12_1$ and, consequently, the crystal is twinned by metric merohedry[23] with a $\bar{4}$ symmetry axis as a twinning element. By considering this kind of twinning, we were able to refine the original structure model and to expand it completely by difference Fourier techniques.

The diffraction data were integrated on the basis of θ-dependent circular integration boxes. The intensities were corrected for Lorenz and polarization factors as well as air scattering.[24] A numerical absorption correction based on face indexing was applied. Merging the data in space

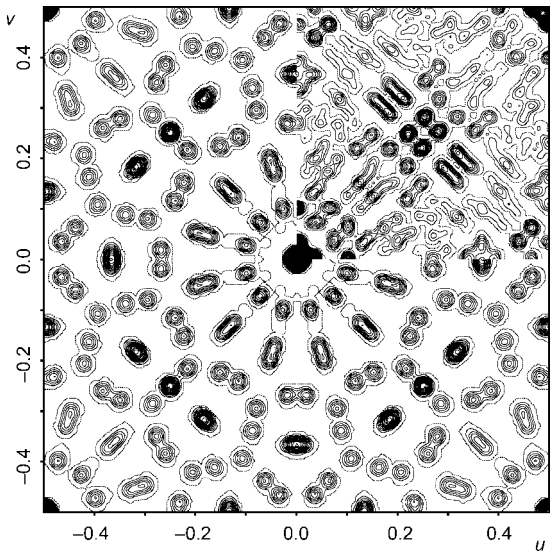

Figure 5. Patterson sections ($uv0$) and ($uv\frac{1}{2}$) (inset: top right) as calculated from the intensities of a twinned crystal of $Ta_{97}Te_{60}$.

group $P2_12_12_1$ yielded 30895 symmetrically independent reflections. In the final cycles of the structure refinement an overall scale factor, an individual scale factor for one of the twin components, and three positional as well as

Table 2. Positional and equivalent isotropic displacement parameters (10^4 pm^2) for $Ta_{97}Te_{60}$.

Atom	x	y	z	U_{eq}
Ta1	0.24174(10)	0.02011(9)	0.66741(14)	0.0337(6)
Ta2	0.11041(9)	0.12720(8)	0.2239(2)	0.0220(6)
Ta3	0.11241(8)	0.15087(8)	0.72554(14)	0.0200(5)
Ta4	0.29762(9)	0.16598(9)	0.2054(2)	0.0233(6)
Ta5	0.43515(9)	0.03311(9)	0.2282(2)	0.0263(7)
Ta6	0.42823(9)	0.05943(9)	0.7074(2)	0.0293(8)
Ta7	0.29564(9)	0.19662(9)	0.7310(2)	0.0312(8)
Ta8	0.43323(10)	0.29948(9)	0.2549(2)	0.0276(7)
Ta9	0.06710(9)	0.33666(9)	0.7307(2)	0.0230(6)
Ta10	0.06128(10)	0.30726(10)	0.2335(2)	0.0323(8)
Ta11	0.42621(9)	0.32959(9)	0.7697(2)	0.0249(7)
Ta12	0.25307(9)	0.34784(9)	0.2589(2)	0.0243(7)
Ta13	0.38261(9)	0.48113(9)	0.2572(2)	0.0265(7)
Ta14	0.11174(9)	0.48453(8)	0.2355(2)	0.0228(6)
Ta15	0.24701(10)	0.38140(10)	0.7457(2)	0.0339(9)
Ta16	0.32092(8)	0.05929(8)	0.22887(14)	0.0203(5)
Ta17	0.31987(8)	0.08155(8)	0.73284(14)	0.0194(5)
Ta18	0.22277(8)	0.08705(8)	0.2267(2)	0.0196(6)
Ta19	0.14865(9)	0.03955(9)	0.7332(2)	0.0199(6)
Ta20	0.15061(9)	0.01641(8)	0.2276(2)	0.0196(6)
Ta21	0.22038(9)	0.11254(9)	0.7352(2)	0.0197(6)
Ta22	0.03448(9)	0.20399(8)	0.19595(14)	0.0191(5)
Ta23	0.03507(8)	0.22729(8)	0.69843(13)	0.0186(5)
Ta24	0.33031(9)	0.27898(9)	0.2100(2)	0.0192(6)
Ta25	0.04127(9)	0.40829(8)	0.2836(2)	0.0222(6)
Ta26	0.04319(9)	0.43597(9)	0.7886(2)	0.0192(6)
Ta27	0.32763(9)	0.30422(9)	0.7127(2)	0.0179(6)
Ta28	0.13875(9)	0.38170(8)	0.2721(2)	0.0217(6)
Ta29	0.35539(9)	0.37691(9)	0.2208(2)	0.0191(6)
Ta30	0.35354(8)	0.40273(8)	0.7212(2)	0.0194(6)
Ta31	0.14154(8)	0.40839(8)	0.7795(2)	0.0191(6)
Ta32	0.39018(8)	0.12574(8)	0.27655(14)	0.0186(5)
Ta33	0.38667(9)	0.15128(8)	0.77855(14)	0.0196(5)
Ta34	0.19424(8)	0.18048(8)	0.2713(2)	0.0187(6)
Ta35	0.05551(9)	0.06805(9)	0.7744(2)	0.0214(6)
Ta36	0.05645(9)	0.04435(8)	0.2712(2)	0.0174(6)
Ta37	0.19402(9)	0.20720(9)	0.7728(2)	0.0197(6)
Ta38	0.46503(8)	0.20000(8)	0.30020(14)	0.0191(5)
Ta39	0.46219(9)	0.22532(8)	0.80395(13)	0.0192(5)
Ta40	0.16818(8)	0.28481(8)	0.2851(2)	0.0184(6)
Ta41	0.45270(9)	0.40317(9)	0.2101(2)	0.0199(6)
Ta42	0.45149(8)	0.43097(8)	0.7100(2)	0.0187(6)
Ta43	0.16746(8)	0.31118(9)	0.7868(2)	0.0195(6)
Ta44	0.13147(8)	0.22912(8)	0.1764(2)	0.0193(6)
Ta45	0.00663(9)	0.10728(8)	0.1767(2)	0.0197(6)
Ta46	0.00799(9)	0.13207(9)	0.6792(2)	0.0180(6)
Ta47	0.13115(9)	0.25545(8)	0.6767(2)	0.0193(6)
Ta48	0.23407(9)	0.25467(9)	0.1804(2)	0.0197(6)
Ta49	0.48171(9)	0.49586(8)	0.8155(2)	0.0180(6)
Ta50	0.48017(9)	0.46823(8)	0.3185(2)	0.0197(6)
Ta51	0.23194(9)	0.28105(9)	0.6817(2)	0.0193(6)
Ta52	0.40082(9)	0.20906(9)	0.1875(2)	0.0194(6)
Ta53	0.47069(8)	0.16125(8)	0.6899(2)	0.0187(6)
Ta54	0.47438(8)	0.13463(8)	0.1903(2)	0.0195(6)
Ta55	0.39772(9)	0.23448(8)	0.6926(2)	0.0191(6)
Ta56	0.21069(8)	0.44983(8)	0.2972(2)	0.0191(6)
Ta57	0.28592(8)	0.44771(9)	0.2002(2)	0.0176(6)
Ta58	0.28566(9)	0.47549(9)	0.6975(2)	0.0192(6)
Ta59	0.21178(8)	0.47878(9)	0.8021(2)	0.0186(6)
Ta60	0.17328(9)	0.06457(9)	0.10697(14)	0.0212(5)
Ta61	0.17160(8)	0.08931(8)	0.61467(14)	0.0216(5)
Ta62	0.27796(9)	0.08828(9)	0.1085(2)	0.0216(6)
Ta63	0.34987(9)	0.03916(9)	0.6109(2)	0.0230(6)
Ta64	0.35529(9)	0.01378(9)	0.1133(2)	0.0217(6)
Ta65	0.27448(9)	0.11590(9)	0.6172(2)	0.0227(6)
Ta66	0.37905(8)	0.11379(9)	0.13716(14)	0.0207(5)
Ta67	0.37474(9)	0.13959(9)	0.64051(14)	0.0206(5)
Ta68	0.20365(9)	0.16137(8)	0.1331(2)	0.0201(6)
Ta69	0.07497(9)	0.03523(9)	0.1342(2)	0.0189(6)
Ta70	0.07378(9)	0.05969(8)	0.6361(2)	0.0190(6)
Ta71	0.20187(9)	0.18796(8)	0.6359(2)	0.0201(6)
Ta72	0.36448(9)	0.22018(9)	0.3189(2)	0.0203(6)
Ta73	0.48823(9)	0.09862(9)	0.3213(2)	0.0207(6)
Ta74	0.48149(9)	0.12544(8)	0.8219(2)	0.0201(6)
Ta75	0.36171(9)	0.25030(9)	0.8238(2)	0.0223(6)
Ta76	0.26542(9)	0.24788(9)	0.3133(2)	0.0199(6)
Ta77	0.48399(9)	0.49940(9)	0.1843(2)	0.0205(6)
Ta78	0.01075(9)	0.47240(9)	0.1826(2)	0.0202(6)
Ta79	0.26298(9)	0.27865(9)	0.8163(2)	0.0224(6)
Ta80	0.09629(9)	0.21321(8)	0.3081(2)	0.0184(6)
Ta81	0.02688(9)	0.16637(8)	0.8117(2)	0.0185(6)
Ta82	0.02350(9)	0.14097(8)	0.3083(2)	0.0212(6)
Ta83	0.09810(9)	0.23817(9)	0.8094(2)	0.0212(6)
Ta84	0.49663(8)	0.26058(8)	0.67931(14)	0.0188(5)
Ta85	0.00072(8)	0.26545(8)	0.82340(14)	0.0200(5)
Ta86	0.33802(8)	0.31986(9)	0.3385(2)	0.0195(6)
Ta87	0.08830(9)	0.42899(9)	0.6616(2)	0.0208(6)
Ta88	0.08295(9)	0.39938(9)	0.1559(2)	0.0240(6)
Ta89	0.33444(9)	0.35098(9)	0.8392(2)	0.0213(6)
Ta90	0.16030(8)	0.32757(9)	0.1567(2)	0.0201(6)
Ta91	0.40738(9)	0.42446(8)	0.8383(2)	0.0210(6)
Ta92	0.40894(9)	0.39408(9)	0.3393(2)	0.0196(6)
Ta93	0.16078(9)	0.35600(9)	0.6589(2)	0.0207(6)
Ta94	0.30965(9)	0.42028(9)	0.3328(2)	0.0209(6)
Ta95	0.18743(8)	0.45481(8)	0.6678(2)	0.0200(6)
Ta96	0.18615(9)	0.42607(9)	0.1635(2)	0.0215(6)
Ta97	0.30909(9)	0.45218(9)	0.8315(2)	0.0196(6)
Te1	0.2551(2)	0.00543(14)	0.7983(2)	0.0359(10)
Te2	0.2397(2)	0.00042(14)	0.0410(2)	0.0433(11)
Te3	0.15326(14)	0.08677(14)	0.3322(2)	0.0262(9)
Te4	0.15106(14)	0.10769(14)	0.8379(2)	0.0249(9)
Te5	0.2857(2)	0.1347(2)	0.3327(3)	0.0269(11)
Te6	0.3762(2)	0.0273(2)	0.3372(3)	0.0340(11)
Te7	0.3961(2)	0.0462(2)	0.8332(3)	0.0277(10)
Te8	0.2864(2)	0.1373(2)	0.8401(3)	0.0331(11)

0947-6539/02/0814-3100 $ 20.00+.50/0 *Chem. Eur. J.* **2002**, *8*, No. 14

Table 2. (Continued).

Atom	x	y	z	U_{eq}
Te9	0.0932(2)	0.1422(2)	0.0934(2)	0.0279(9)
Te10	0.0932(2)	0.1697(2)	0.5963(2)	0.0276(9)
Te11	0.3179(2)	0.2217(2)	0.0982(3)	0.0285(10)
Te12	0.4882(2)	0.0780(2)	0.6025(3)	0.0353(11)
Te13	0.4701(2)	0.0456(2)	0.1046(3)	0.0331(11)
Te14	0.3089(2)	0.2294(2)	0.6067(3)	0.0348(12)
Te15	0.4480(2)	0.2897(2)	0.3861(3)	0.0359(12)
Te16	0.0485(2)	0.3023(2)	0.6053(3)	0.0300(11)
Te17	0.0571(2)	0.2839(2)	0.1050(3)	0.052(2)
Te18	0.4594(2)	0.3086(2)	0.8954(3)	0.0318(11)
Te19	0.2043(2)	0.3614(2)	0.3756(3)	0.0305(11)
Te20	0.3803(2)	0.4558(2)	0.1265(3)	0.0271(10)
Te21	0.3746(2)	0.46697(14)	0.6175(3)	0.0280(11)
Te22	0.2171(2)	0.3838(2)	0.8740(3)	0.0342(12)
Te23	0.0771(2)	0.3222(2)	0.3623(3)	0.0449(14)
Te24	0.4094(2)	0.3214(2)	0.1265(3)	0.0371(12)
Te25	0.4183(2)	0.3367(2)	0.6365(3)	0.0270(10)
Te26	0.0769(2)	0.3457(2)	0.8636(3)	0.0273(10)
Te27	0.1162(2)	0.4684(2)	0.3678(3)	0.0287(11)
Te28	0.2690(2)	0.3531(2)	0.1269(3)	0.0338(12)
Te29	0.2816(2)	0.3670(2)	0.6203(3)	0.043(2)
Te30	0.1117(2)	0.4766(2)	0.8796(3)	0.0340(12)
Te31	0.35122(14)	0.0860(2)	0.0137(2)	0.0268(9)
Te32	0.3437(2)	0.11040(14)	0.5162(2)	0.0275(9)
Te33	0.2176(2)	0.1266(2)	0.0092(3)	0.0263(10)
Te34	0.1103(2)	0.0191(2)	0.0110(2)	0.0277(10)
Te35	0.1171(2)	0.0478(2)	0.5121(3)	0.0258(10)
Te36	0.2156(2)	0.1423(2)	0.5129(3)	0.0266(10)
Te37	0.04678(14)	0.19088(13)	0.4237(2)	0.0248(9)
Te38	0.04842(14)	0.21557(14)	0.9267(2)	0.0243(8)
Te39	0.3147(2)	0.2493(2)	0.4322(3)	0.0255(10)
Te40	0.01631(14)	0.4498(2)	0.5671(3)	0.0244(10)
Te41	0.0120(2)	0.4222(2)	0.0633(3)	0.0258(10)
Te42	0.3129(2)	0.2801(2)	0.9353(3)	0.0281(10)
Te43	0.3472(2)	0.3827(2)	0.4474(3)	0.0275(10)
Te44	0.14925(14)	0.41625(14)	0.5511(2)	0.0226(9)
Te45	0.1454(2)	0.3903(2)	0.0474(3)	0.0269(10)
Te46	0.3470(2)	0.4110(2)	0.9478(3)	0.0249(10)
Te47	0.42024(13)	0.15161(14)	0.4037(2)	0.0230(8)
Te48	0.41167(14)	0.17795(14)	0.9053(2)	0.0217(8)
Te49	0.1798(2)	0.22383(13)	0.3930(2)	0.0216(9)
Te50	0.01718(14)	0.08174(14)	0.8977(3)	0.0237(10)
Te51	0.01599(14)	0.05728(13)	0.3956(3)	0.0226(10)
Te52	0.1816(2)	0.2464(2)	0.8941(3)	0.0238(10)
Te53	0.44949(14)	0.1819(2)	0.0727(2)	0.0250(9)
Te54	0.44313(14)	0.20800(14)	0.5739(2)	0.0227(8)
Te55	0.1846(2)	0.2518(2)	0.0629(3)	0.0277(10)
Te56	0.48247(14)	0.44573(14)	0.9355(3)	0.0238(10)
Te57	0.4831(2)	0.41763(14)	0.4368(3)	0.0252(10)
Te58	0.1822(2)	0.27913(14)	0.5612(2)	0.0234(9)
Te59	0.25073(14)	0.48262(14)	0.4166(2)	0.0244(10)
Te60	0.2511(2)	0.48591(14)	0.0818(2)	0.0226(9)

six anisotropic displacement parameters for the 157 crystallographic independent atoms were refined against 30458 intensities with $I>0$ minimizing the expression $\Sigma w(F_o^2-F_c^2)^2$, $w=\{\sigma^2(F_o^2)+[0.06(2F_o^2+\max(F_o^2,0))/3]^2\}^{-1}$. Anomalous dispersion effects were taken into account. Assuming additional twinning by inversion in the refinement resulted in negligible additional twin fractions. A final difference Fourier analysis revealed a maximal residual electron density 120 pm apart from Ta50. None of the twenty strongest peaks was located in a gap between the sheets of Te atoms. Thus, intercalation of $Ta_{97}Te_{60}$ by additional Ta can be ruled out. The final atomic parameters are given in Table 2.

Further details of the single crystal structure refinement may be obtained from the Fachinformationszentrum Karlsruhe, D-76344 Eggenstein-Leopoldshafen, Germany (fax: (+49) 7247-808-666; e-mail: crysdata@fiz-karlsruhe.de), on quoting the depository number CSD-412293.

Acknowledgements

This work was financially supported by the Deutsche Forschungsgemeinschaft and the Fonds der Chemischen Industrie. A generous donation of tantalum by H. C. Starck is gratefully acknowledged. The authors thank Dr. Hahn, the company of Stoe, for the acquisition of a set of intensity data, and Dr. Krumeich for the EDX analyses.

[1] a) D. Levine, P. J. Steinhardt, *Phys. Rev. Lett.* **1984**, *53*, 2477–2480; b) C. Janot, *Quasicrystals, A Primer*, Clarendon, Oxford, **1992**; c) *Lectures on Quasicrystals* (Eds.: F. Hippert, D. Gratias), Les Edition de Physique Les Ulis **1994**; d) "Quasicrystals": *Mater Res. Soc. Symp. Proc.* **1999**, *553*; e) "Proceedings of the 7th International Conference on Quasicrystals", *Mater. Sci. Eng. A* **2000**, *294–296*.

[2] a) W. Steurer, *Z. Kristallogr.* **1990**, *190*, 179–234; b) A. Yamamoto, *Acta Crystallogr. Sect. A.* **1996**, *52*, 509–560.

[3] a) N. G. de Bruijn, *Nederl. Akad. Wetensch. Indag. Math.* **1981**, *43*, 39–52; b) N. G. de Bruijn, *Nederl. Akad. Wetensch. Indag. Math.* **1981**, *43*, 53–66; c) M. Dunot, A. Katz, *Phys. Rev. Lett.* **1985**, *54*, 2688–2691; d) V. Elser, *Phys. Rev. B*, **1985**, *32*, 4892–4898; e) P. A. Kalugin, A. Yu. Kitaev, L. C. Levitov, *JETP Lett.* **1985**, *41*, 145–149; f) P. Bak, *Phys. Rev. Lett.* **1986**, *56*, 861–864; g) T. Janssen, *Acta Crystallogr. Sect. A.* **1986**, *42*, 261–271.

[4] a) S. E. Burkov, *Phys. Rev. Lett.* **1991**, *67*, 614–617; b) S. E. Burkov, *J. Phys.* **1992**, *2*, 695–706; c) M. Duneau, *Quasicryst. Proc. Int. Conf. 5th* **1995**, 116; d) P. Gummelt, *Geometriae Dedicata* **1996**, *62*, 1–17; e) P. J. Steinhardt, H.-C. Jeong, K. Saitoh, M. Tanaka, E. Abe, A. P. Tsai, *Nature* **1998**, *396*, 55–57.

[5] a) F. Krumeich, M. Conrad, B. Harbrecht, *Electron Microsc. 1994 Proc. Int. Congr. Electron Microsc. 13th* **1994**, *2*, 752; b) M. Conrad, PhD thesis, Universität Dortmund (Germany) **1997**; c) M. Conrad, B. Harbrecht, F. Krumeich, *Aperiodic 97 Proc. Int. Conf. Aperiodic Cryst.* **1998**, 199–203; d) M. Conrad, F. Krumeich, B. Harbrecht, *Angew. Chem.* **1998**, *110*, 1453–1457; *Angew. Chem. Int. Ed.* **1998**, *37*, 1383–1386; e) F. Krumeich, M. Conrad, H.-U. Nissen, B. Harbrecht, *Philos. Mag. Lett.* **1998**, *78*, 257–367; f) M. Uchida, S. Horiuchi, *Jpn. J. Appl. Phys.* **1997**, *36*, L1523–1524; g) M. Uchida, S. Horiuchi, *J. Appl. Crystallogr.* **1998**, *31*, 634–637.

[6] a) T. Ishimasa, H.-U. Nissen, Y. Fukano, *Phys. Rev. Lett.* **1985**, *55*, 511–513; b) C. Beeli, F. Gähler, H.-U. Nissen, P. Stadelmann, *J. Phys.* **1990**, *51*, 661–674.

[7] a) H. Chen, D. X. Li, K. H. Kuo, *Phys. Rev. Lett.* **1988**, *60*, 1645–1648; b) K. H. Kuo, Y. C. Feng, H. Chen, *Phys. Rev. Lett.* **1988**, *61*, 1740–1743.

[8] a) K. Yoshida, T. Yamada, Y. Taniguchi, *Acta Crystallogr. Sect. B* **1989**, 40–45; b) K. Yoshida, T. Yamada, Y. Taniguchi, *Phil. Mag. Lett.* **1991**, *63*, 127–132; K. Yoshida, *Mater. Sci. Forum* **1994**, *150–151*, 129–138.

[9] D. Xu, Y. Song, W. Su, H. Lin, *Gaoya Wuli Xuebao* **1994**, *8*, 60–64.

[10] a) F. C. Frank, J. S. Kasper, *Acta Crystallogr.* **1958**, *11*, 184–191; b) F. C. Frank, J. S. Kasper, *Acta Crystallogr.* **1959**, *12*, 483–499; c) Y. P. Yarmolyuk, P. I. Kripyakevich, *Sov. Phys. Crystallogr.* **1974**, *19*, 334–337; d) D. P. Shoemaker, C. B. Shoemaker, *Acta Crystallogr. Sect. B*, **1986**, *42*, 3–11.

[11] G. Bergman, P. Shoemaker, *Acta Crystallogr.* **1954**, *7*, 857–865.

[12] A. Simon, *Angew. Chem.* **1981**, *93*, 23–44; *Angew. Chem. Int. Ed. Engl.* **1981**, *20*, 1–22;

[13] a) H. E. S. Socolar, T. C. Lubensky, P. J. Steinhardt, *Phys. Rev. B* **1986**, *34*, 3345–3360; b) P. Stampfli, *Helv. Phys. Acta* **1986**, *59*, 1260–1263; c) F. Gähler, PhD thesis, ETH Zürich (Switzerland), **1988**.

[14] a) M. Conrad, B. Harbrecht, *Aperiodic 97 Proc. Int. Conf. Aperiodic Cryst.* **1998**, 205–209; b) F. Krumeich, M. Conrad, B. Harbrecht, *Aperiodic 97 Proc. Int. Conf. Aperiodic Cryst.* **1998**, 211–215; c) M.

Uchida, S. Horiuchi, *Jpn. J. Appl. Phys.* **1998**, *37*, L531 – 532; d) "Quasicrystals":C. Reich, M. Conrad, F. Krumeich, B. Harbrecht, *Mater Res. Soc. Symp. Proc.* **1999**, *553*, 83 – 94; e) M. Conrad, F. Krumeich, C. Reich, B. Harbrecht, *Mater. Sci. Eng. A* **2000**, *294 – 296*, 37 – 40; f) F. Krumeich, C. Reich, M. Conrad, B. Harbrecht, *Mater. Sci. Eng. A* **2000**, *294 – 296*, 152 – 155;

[15] H. Q. Ye, D. X. Li, K. H. Kuo, *Acta Crystallogr. Sect. B* **1984**, *40*, 461 – 466.

[16] D. X. Li, K. H. Kuo, *Acta Crystallogr. Sect. B* **1986**, *42*, 152 – 159.

[17] B. Boren, *Ark. Kemi. Mineral. Geol.* **1933**, *11A*, 1 – 28.

[18] C. Wilson, *Acta Crystallogr.* **1960**, *13*, 56 – 57.

[19] J. Bohm, K. Dornberger-Schiff, *Acta Crystallogr.* **1967**, *23*, 913 – 933.

[20] For the benefit of the reader unfamiliar with this term we give a definition: a layer group is a complete set of symmetry operations under which a three-dimensional object exhibiting translational symmetry in only two dimensions is invariant. The symbol in parentheses refers to the crystallographic direction in which the object lacks translational symmetry.

[21] G. M. Sheldrick, *Acta Crystallogr. Sect. A*, **1990**, *46*, 467 – 473.

[22] T. Debaerdenmaeker, G. Germain, P. Main, C. Tate, M. M. Woolfson, Multan 88, A System of Computer Programs for the Automated Solution of Crystal Structures from X-ray Diffraction Data, University of York (UK), **1988**.

[23] N. Nespolo, G. Ferraris, *Z. Kristallogr.* **2000**, *215*, 77 – 81.

[24] Program Package for X-ray Diffraction, Version 2.75, Stoe, Darmstadt (Germany), **1996**.

[25] G. M. Sheldrick, SHELXL 93, Program for the Refinement of Crystal Structures, University of Göttingen, **1993**.

[26] M. Conrad, B. Harbrecht, *J. Alloys Compd.* **1992**, *187*, 181 – 192.

Received: January 3, 2002 [F3774]

  0947-6539/02/0814-3102 $ 20.00+.50/0